International Journal of Research
Available at https://edupediapublications.org/journals
e-ISSN: 2348-6848
p-ISSN: 2348-795X
Volume 05 Issue 12
April 2018

A NOVEL CASCADE TEMPERATURE CONTROL SYSTEM FOR HIGH-SPEED HEAT-AIR FLOW WIND TUNNEL

Kondiba R. Gayake
PG Department
M. B. E. Society's College Of Engineering Ambajogai
Ambajogai, India
Email:-Kondibagaikegaike21@Gmail.com

S.S.Sankeswari
PG Department
M. B. E. Society's College Of Engineering Ambajogai
Ambajogai, India
Email:-sankeswari@Gmail.com

Abstract — **In order to meet stringent temperature-control requirements in a high-speed airflow wind tunnel (HAWT) for thermal simulation under complicated work conditions such as thermal strength experiment of aero engine blade and dynamic calibration of high temperature thermal coupler, this paper proposes a novel cascade fuzzy-PID (C-Fuzzy-PID) compound control method for regulating the fuel-oil flow rate in the inner loop and temperature in the outer loop. The mathematical models that characterize the dynamics of the heat airflow temperature in the combustor and the fuel-oil flow rate for combustion are derived, upon which the improved PID control laws for the inner and outer loops are described. The former employs a fuzzy-PID controller with a predictor for controlling flow rate in the inner loop, which effectively overcomes influences according to its characteristics of large inertia and transport lag in fuel-oil supply system on the temperature responses. The latter combines disturbance compensation and a fuzzy-PID feedback law to suppress influences due to factors such as change in work conditions, disturbances, and time-varying parameter variations. The C-Fuzzy-PID method has been numerically investigated by comparing simulation results against two traditional PID-based methods, as well as experimentally validated confirming that the proposed control algorithm has strong robustness and excellent adaptability for temperature control of an HAWT.**

Keywords—Cascade control, fuzzy PID, high-speed heat airflow Simulation, predictive control, temperature control, thermal.

I. INTRODUCTION

The high-speed airflow wind tunnel (HAWT) for thermal Simulation is an important aerospace experimental system. An HAWT that produces a uniform and controllable temperature field has been widely used in heat-strength experiments of High temperature aero engine blades and dynamic calibration of Thermal sensors. Among the challenges in developing an HAWT is the modeling of the dynamic system and the design of a controller capable of regulating temperature and fuel oil with Quick response for a wide range of the temperature.

The mixing of the aviation kerosene with air and their subsequent burning in the combustor results in a complex physical field; the thermal-flied environment being simulated is a high-speed airflow of high temperature. The high temperature airflow field is governed by the flow rate ratio between the Kerosene and the air supplied to the combustor. In practice, the Outlet airflow temperature of the HAWT for a specified airflow Speed is adjustable when conducting experiments. Thus, the output temperature of the combustor, which depends primarily on kerosene flow rate, can be theoretically controlled by precisely manipulating the flow rate of the fuel oil feeding to the combustor. However, variations in the input airflow along With inadequate fuel-oil combustion and other unknown factors Result in significant temperature fluctuations which must be considered in the controller design for regulating fuel-oil flow Rate and temperature. Prior research generally focused on the Design and control of thermal wind tunnels particularly on three Aspects: modeling and regulating the flow rate, developing a Strategy for controlling flow rate, and designing a temperature Control system for the combustion process.

II MODELING OF TEMPERATURE CONTROL SYSTEM

This paper addresses problems commonly encountered in designing a controller for simultaneously regulating both the fuel-oil flow rate and the temperature of an HAWT, where the plant is characterized by a wide temperature range from 200 to 1700 ◦C and high heating rate (with temperature raised from 200 to 1700 ◦C within 30 s). Additionally, the control law must be able to deal with large thermal and flow inertia, transport time lag, and robust in the presence of significant disturbances. To effectively solve these problems, there is a need to develop a mathematical model that takes into accounts the combined dynamics of fuel-oil flow and combustion, and a method for high-performance temperature control with strong robustness. The rest of this paper offers the following.

1) The mathematical models that characterize the dynamics of fuel-oil flow and the gas temperature in the combustor for a typical HAWT are derived, which provide the essential basis for design analysis and numerical simulation.

2) Along with the new approach for regulating the flow rate of the fuel-oil supply system, a new C-Fuzzy-PID control law (consisting an inner flow rate and an outer temperature Fig. 1.

International Journal of Research
Available at https://edupediapublications.org/journals
e-ISSN: 2348-6848
p-ISSN: 2348-795X
Volume 05 Issue 12
April 2018

Temperature control system of HAWT. Control loops) is presented. The inner loop incorporates a Predictive control law to overcome the influences of transport lag in the fuel-oil supply system while the outer loop is designed to suppress disturbances due to the wind speed change. Compared with the traditional PID cascade control, the C-Fuzzy-PID effectively rejects to the influence of the time lag and working conditions change.

3) The C-Fuzzy-PID method has been numerically studied by comparing simulation results against two traditional methods, PID-PID and PID-Smith, as well as experimentally evaluated demonstrating its robustness and excellent adaptability.

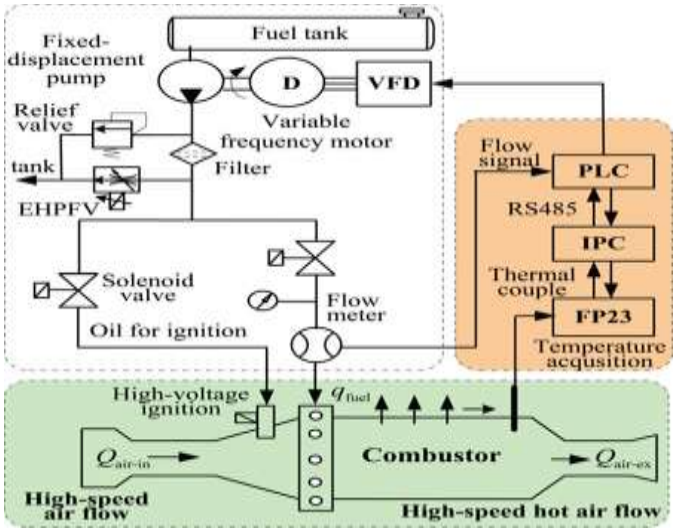

Fig.1. Temperature control system of HAWT.

Fig. 2 shows the temperature control system of a typical HAWT, which consists of three subsystems; fuel-oil supply, combustion, and computer control. The fuel-oil supply subsystem adjusts the flow rate of the aviation kerosene feeding to the combustor. The combustion subsystem mixes the fogged kerosene with preheated air, burns them, and finally forms the heat air flow at a specified temperature. The control subsystem consists of a programmable logic controller (PLC) as a field controller, an industrial personal computer (IPC) as a remote controller, flow rate sensors, thermocouples, VF driver, and signal conditioning circuits. Specific control algorithms are implemented on the IPC considering that the operation ability of the PLC is limited. The PLC receives control commands from the IPC, adjusts the fuel-oil flow rate through controlling the VF motor and the proportional valve, and finally achieves the closed-loop temperature control of the overall system.

III DESIGN OF THE CONTROLLERS

I .Modeling of Flow Rate in the Inner Loop

Because the fuel-oil supply system is mainly operated in the VF speed-regulating mode, the mathematical model and flow rate control strategy have been setup in this mode. The operation mode of VFD in this system is variable voltage variable frequency, the input control signal is the output voltage of the controller, and the output of the VFD is the voltage across to the stator coil of the VF induction motor. The relationship between input and output of the VFD is linear; when not considering low frequency torque compensation, it can be expressed by

$$U_A = K_f K_{inv} u \qquad (1)$$

Where UA is the output voltage of VFD

K_f is the gain between the frequency f and the input control voltage u of the VFD, and K_{inv} is the voltage–frequency ratio. Generally, the VF induction motor is operated with a constant voltage–frequency ratio, where the electromagnetic time constant is much smaller than that of rotor dynamics. Denoting ωs as the synchronized angular frequency of the motor, Rs as the phase resistance of the stator side, and Ls and L_{re} as the stator inductance and equivalent rotor inductance, respectively, and considering that the slip ratio ($S_L = 1 - n_p/n_s$) of the asynchronous motor is usually less than 5% under the common work conditions,

Therefore $Rre \gg sLR_s, R_{re} \gg sL\omega_s(L_s + L_{re})$. Under the aforementioned conditions, the torque Γ_e (in N · m) acting on the motor shaft, which can be derived from the electromagnetic moment equation of the VF motor, can be approximately written as

$$T_e \approx \frac{3m_p U^2 A}{W_S R_{re}} SL = \frac{3m_p U^2 A}{2\pi R_{re}} SL \qquad (2)$$

Where $\omega_s = \pi ns/30$; ns = 60f/mp; n_s and ns are the actual rotational speed and the synchronous rotational speed of the motor in revolution per minute, respectively. Substituting the expressions of sL and ns into (2) yields

$$T_e = \frac{3m_p}{2\pi R_{re}} K_f U_A - \frac{m^2 p}{40\pi Rre} K^2 f n_p = K_1 U_A - K_2 n_p \qquad (3)$$

Mechanically, the moment balance equation on the motor shaft is as follows

$$T_e = J_T \frac{\pi}{30}\frac{dnp}{dt} + B_T \frac{\pi n_p}{30} + \frac{D_P P_P}{2\pi n_{pm}} \qquad (4)$$

Where P_p is the output pressure of the pump in Pascal.

According to the continuity equation describing the flow rate of the volumetric chamber in the output port of the pump, and neglecting the influence of the compressibility of the fuel oil while considering that the pressure of the fuel oil is less than 1.2 MPa and the volume elastic modulus of fuel oil is larger than1.0 GPa.

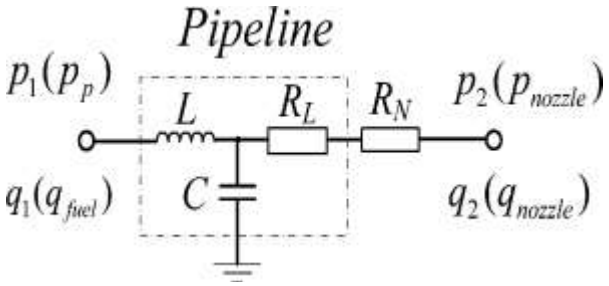

Fig.2. Lumped-parameter model of a long pipeline.

The output flow rate of the oil supplying the pump can be approximately written as follows:

$$q_{fuel} = \frac{1}{60} D_P n_p - C_P P_p \qquad (5)$$

International Journal of Research
Available at https://edupediapublications.org/journals
e-ISSN: 2348-6848
p-ISSN: 2348-795X
Volume 05 Issue 12
April 2018

Where q_{fuel} is actual flow rate of oil supplying pump, m3/s. Since the energy loss of the long fuel-oil pipeline from the pump to the combustor nozzle of the HAWT is the pressure loss, it must be modeled to account for its influences. Moreover, there are also dynamic influences of the fluid inductance and capacitance of the pipeline, as well as the throttling resistance of the nozzle in the combustor. Using the lumped parameter method [13] to model the long pipeline system (in terms of its fluid resistance R, capacitance C, and inductance L as shown in Fig. 3), the equation characterizing the transfer functions of the pipeline can be written as

$$\begin{bmatrix} P_2(s) \\ q_2(s) \end{bmatrix} = \begin{bmatrix} 1+LCs^2 & -(1+Ls+RLCs^2) \\ -Cs & 1+RCs \end{bmatrix} \begin{bmatrix} P_1(s) \\ q_1(s) \end{bmatrix} \quad (6)$$

Where $C = \frac{\pi d^2 l}{4\beta e}$; $L = \frac{4\rho_{fuel}}{\pi d^2 4\beta e} l$; $R = R_1 + R_2$, $R1 = \frac{128\mu l}{\pi d^4}$,R_i and R_2 are the liquid resistance of the pipeline liquid or the nozzle, respectively. The resistance R_N of the nozzle. Is obtainable from linearizing its pressure/flow rate relationship:

$$q_2 = C_d A\sqrt{2} p_{2/\rho_{fuel}} \quad (7)$$

Where C_d is the discharge coefficient, and A is the effective flow area of the hole. Linearizing (7) about the operating spout pressure $\overline{p_2}$ (which is generally a measurement value at starting Frequency) leads to (8) for a constant area nozzle hole

$$\Delta q_2 = Kc\Delta p_2 \text{ where } K_c = \frac{C_d \bar{A}}{\sqrt{2\rho_{fuel}\overline{P_2}}} \quad (8)$$

There are six nozzles in the combustor, and the liquid resistance at the spout can be obtained according to the principle of resistance parallel as follows:

$$R_2 = \frac{1}{6K_c} = \frac{1}{6}\frac{\partial p_2}{\partial q_2} = \frac{\sqrt{2\rho_{oil}\overline{P_2}}}{6C_d A} \quad (9)$$

Neglecting the compressibility of fuel oil and considering C = 0 in (6), and we can obtain.

$$q_1 = q_2 = q_{fuel} = \frac{P_p}{L_s + R_1 + R_2} \quad (10)$$

Combining (1) to (10) yields a transfer function between the oil fuel flow rate q_{fuel} and the VFD input voltage u as follows:

$$G_0(s) = \frac{q_{fuel}(S)}{u(S)} = \frac{b_0 \omega^2_n}{s^2 + 2\zeta\omega_n s + \omega^2_n} \quad (11)$$

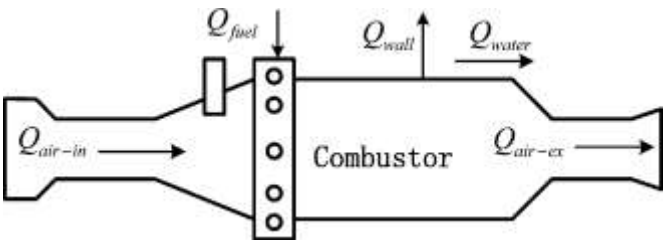

Fig. 3. Energy transfer diagram in a combustor

Where $\omega^2 n = \frac{1}{J_T c_p L}(1 + C_p R)\left(B_T + \frac{30}{\pi} K_2\right)\frac{d^2_p R}{40\pi^2 n_m c_p}$; $2\ \omega_n = \frac{1}{J_T}\left(B_T + \frac{d^2_p}{40\pi^2 n_m c_p}\right) + \frac{1+C_p R}{c_p L} + (1 + C_p R) + \frac{30}{\pi} K_2$; and $B_0 \omega^2{}_n = \frac{K_1 d_p}{2\pi J_T c_p L}$.

To account for the pure time delay τ existed in gear flow meter, the output flow rate qs of the flow meter is expressed by

$$q_s(s) = e^{-\tau s} q_{fuel}(s) \quad (11a)$$

II. Modeling of Temperature in the Outer Loop

Fig. 4 illustrates the energy transfer in the combustor, where the gas temperature in the combustor is the controlled variable in the outer loop. Formulated using a lumped parameter approach, the gas temperature T (assumed uniform in the combustor) is governed by the law of energy conservation given in (12) along with the individual contributions of the heat powers Q (W) defined in (12a)–(12e) in terms of temperatures (◦C):

$$V\rho_{p c_p}\frac{dT}{dt} = Q_{fuel} + Q_{air-in} - (Q_{air-ex+Q_{water}}\ Q_{wall}) \quad (12)$$

$$Q_{fuel} = H\rho_{fuel} q_{fuel} \quad (12a)$$

$$Q_{air-in} = \rho_{air-in} q_{air-in} C_{p1} T_{in} \quad (12b)$$

$$Q_{air-ex} = \rho_e q_{ex} C_{Pe} T \quad (12c)$$

$$Q_{wall} = hA_c(T_f - T_\infty) \quad (12d)$$

And

$$Q_{water} = \rho_\omega q_\omega C_\omega (T_\omega - T_{\omega 0}) \quad (12e)$$

Where Q_{oil} the heat power is released by combustion of the fuel oil into the combustor; Q_{air-in} and Q_{air-ex} are the heat power brought into and out the combustor by the airflow and the exhaust gas, respectively; Q_{wall} and Q_{water} are the power due to conduction heat transfer through the combustor wall and that due to heat circulation of the cooling water, respectively. Tin is the temperature of the airflow entering the combustor; T_f is the temperature of the inner combustor wall; T∞ is the ambient temperature; $T_{\omega 0}$ and T_ω are the temperature of the cooling Water flowing into and out of the combustor, respectively; andρ_e, q_{ex} , and C_{Pe} are the density (kg/m3), flow rate (m3/s), and specific heat capacity (J/Kg°C) of the exhaust gas flowing out of the combustor. Substituting (12a)–(12e) into (12) yields

$$V\rho_{p c_p}\frac{dT}{dt} = H\rho_{fuel} q_{fuel} + \rho_{air-in} q_{air-in} C_{P1} T_{in} - \rho_{ex} q_{ex} c_{p2} T - KA_1(T_{f-} T_\infty) - \rho_\omega q_\omega C_\omega (T_\omega - T_{\omega 0}). \quad (13)$$

According to the law of quality conservation (with negligible quality change of gas in the combustor), we have

$$\rho_{ex} q_{ex} = \rho_{fuel} q_{fuel} + \rho_{air-in} q_{air-in}. \quad (14)$$

The mass flow rate of the input air $\rho_{air-in} q_{air-in}$ is much larger than the mass flow rate of the oil fuel $\rho_{fuel} q_{fuel}$ in the actual burning process. So, we can consider$\rho_{ex} q_{ex} \approx \rho_{air-in} q_{air-in}$, and also can consider $C_{p1} \approx C_{P2} \approx C_p$. Assume that the temperature of combustor wall$T_f = \alpha T$ and cooling water temperatures in export Tω = βT, then (13) can be simplified as

$$V\rho_{p c_p}\frac{dT}{dt} + \rho_{fuel} q_{fuel} + \rho_{air-in} q_{air-in} C_P T_{in} + KA_1 \alpha T_\infty + \rho_\omega q_\omega C_\omega \beta T = H\rho_{fuel} q_{fuel} + \rho_{air-in} q_{air-in} C_P T_{in} + KA_1 T_\infty + \rho_\omega q_\omega C_\omega T_{\omega 0}. \quad (15)$$

International Journal of Research
Available at https://edupediapublications.org/journals
e-ISSN: 2348-6848
p-ISSN: 2348-795X
Volume 05 Issue 12
April 2018

Because the inlet air, the inlet temperature, cooling environmental Temperature of combustor wall, and temperature of the cooling water are basically stable and can be seen as a constant in the experimental process for the certain work conditions, so the rear three items of (15) can be considered as a constant item. Taking Laplace transformation of (15) leads to the transfer function between T(s) and $q_{oil}(s)$ as follows:

$$G_1(s) = \frac{T(S)}{q_{oil}(S)} = \frac{K_p}{T_p s + a} \qquad (16)$$

Where $a = \rho_{air-in} q_{air-in} C_P + KA_1\alpha + \rho_\omega q_\omega C_\omega \beta, K_P = H\rho_{fuel}$, and $T_p = V\rho_{p c_p}$.

III. PROPOSED CONTROLLERS

The following two sections describe the design of the inner and outer loop controllers for regulating the fuel-oil flow rate and gas temperature, respectively

I. Design of a Flow Rate Controller in the Inner Loop

As modeled in (11) and (11a) and observed during the debugging of the system, the open-loop transfer function of the inner loop control system has a transport lag due to the flow rate sensor. In addition, the nonlinearity and uncertainty of the motor pump and pipeline also makes it difficult to achieve the desired control effects by simply using a simple fixed-gain PID controller. Fuzzy control law and fuzzy rule-based control law have been widely applied in control systems because it relaxes the accuracy requirements on the mathematical model of the plant. According to the system characteristics of a typical HAWT, an improved fuzzy-PID controller with a predictive algorithm is designed for the flow rate control in the inner loop as shown in Fig. 5. This new compound fuzzy PID control law is effective in overcoming the effects of time delay on the system. The fuzzy-PID predictive controller achieves its control performance through the combined effects of predictive control on the time-delay elimination and rule-based tuning PID gains on the improved system robustness and steady-state accuracy. As illustrated in Fig. 5, the fuzzy-PID predictive controller is implemented in three steps. In the first step, a Levinson predictor is designed to determine the output value of the future d steps from the historical data of the process output. Next, the error is computed by comparing the predicted value that is fed back

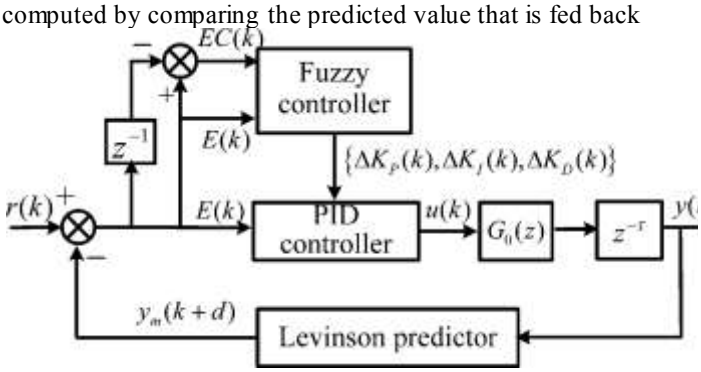

Fig.4. Fuzzy PID predictive controller

Against the reference signal. Based on the computed error and the PID gain parameters that are updated by the fuzzy controller in real time, the final step determines the output of the PID Controller.

I. Levinson Predictor: The Levinson predictor method predicts the values of the output variables in the future d steps built upon the moving output average y_m of n process historical data. For the predictor output at kth time instant in (17), the predicted value of d step ahead is given by (18)

$$y_m(k) = -\sum_{i=1}^{n} aiy(k-i) \qquad (17)$$

Where $y_m(k+d\ k) = -a_1 y_m(k+d-1\ k) - \cdots$
$-a_{p-1} y_m(k+1\ k) - a_p y(k) - \cdots$
$- a_n y(k+d-n)$. (18)

In (17) and (18), the optimal forecasting parameters, {ai} where i = 1... n, are predetermined using a recursive least squares method

II Design of a Fuzzy-PID Controller:

The three PID gains are generally determined through empirical methods such as process reaction curve criteria; once determined, they cannot be changed throughout the controlling process. Unfortunately, these simple fixed-gain PID controllers will not guarantee the adaptability of the actual fuel supply system to the change of its working conditions. In order to have a good control effect on the flow rate, this paper enhances the PID controller with fuzzy control which adjusts in real time the PID gains according to the state of the linguistic variables (E and EC) of the error e and the error change ec; namely, the inputs of the fuzzy PID Controllers are e and ec, and the output is the three incremental gains (ΔKp, ΔKi, and ΔKd) of the PID control law. When implementing the fuzzy PID control law, the controller inputs (e and ec) are quantified to the specified range (−5, 5), upon which the membership degree for each linguistic variable is then determined. Here, the linguistic variable sets for the inputs and output of the fuzzy controller are chosen as {NB, NM, NS, ZO, PS, PM, PB} and expressed by {−4, −3, −2, −1, 0, 1, 2, 3, 4}. Unlike the traditional fuzzy control a Mamdanni's rule table for fuzzy reasoning, the fuzzy rules for the fuzzy-PID controller are based on analytic formula with an adjusting factor to improve $A = \pi r^2$ the adaptability of the fuzzy rule as follows:

$$U = [\ E + (1 - \ )EC] \qquad (19)$$

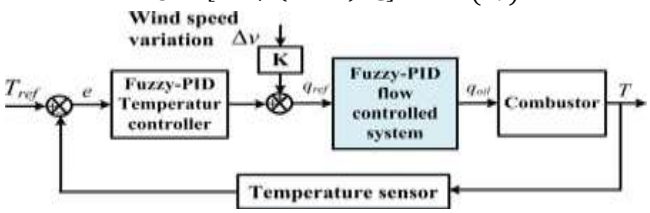

Fig.5. Structure of an outer loop temperature controller

Where λ is the correction factor, its adjustment law is

$$= \ _1 E \ _2 , \ _1, \ _2 \in [0,1] \qquad (20)$$

Where λ1 and λ2 are selected according to the impact weights of the error on the control system performance. Using (19), the output of the fuzzy PID controller is calculated, upon which the incremental PID gains are determined with a defuzzier.

International Journal of Research
Available at https://edupediapublications.org/journals
e-ISSN: 2348-6848
p-ISSN: 2348-795X
Volume 05 Issue 12
April 2018

The fire-membership function $\mu_F(u)$ for the fuzzy control output of each fuzzy rule can be determined as

$$\mu_F(u) = A = \sum_{i=1}^{5}\sum_{j}^{5} \mu_{(i,j)}(\mu)_{\mu i}(e)_{\mu j}(ec) \qquad (21)$$

Where μi (e), μj (ec), and μ (i,j)(u) denote the triangular membership functions. Calculation of the defuzzier formula (based on the method in [30] and [31]) can be written as

$$\mu = \sum_{k=-5}^{5} \mu_F(\mu_k)\,\mu_k \Big/ \sum_{k=-5}^{5} \mu_F(\mu_k) \qquad (22)$$

Where u denotes the output of the fuzzy controller after defuzzier and it has three gains of fuzzy PID.

II. Design of Temperature Controller in the Outer Loop

As seen in (15), changes of the airflow, cooling water flow Rate and environment temperature would appear as disturbances in the combustor gas-temperature control system. Because the flow rate of the cooling water can be adjusted by a water supply with a regulating valve and a water pump with a fixed rotational speed in practice, the change in flow rate of the cooling water is not large. On the other hand, temperature experiments with different wind speeds at the same temperature are often needed. For example, the characteristics of a specimen at a specific temperature (say 1000◦C) must be tested for a range of wind speeds (say 0.6, 0.8, and 1 Ma). Any switch in wind speed could have a significant influence on the model and control performance of the plant; thus, the control system not only must reject any disturbances quickly to achieve accurate temperature regulation, but also overcome any impact caused by a switch of work condition; for example, a change in the airflow from 0.6 to 0.8 Ma In order to accomplish this control objective, a compound controller has been designed as shown in Fig. 6, which combines compensation for wind speed change with a fuzzy PID for temperature control. The fuzzy-PID temperature controller has the same structure for the fuzzy-PID flow rate controller in the inner loop. The compensation coefficient to reflect the Change of the wind speed is determined by combustion theory and empirical experience.

IV. SIMULATION AND RESULTS

In last chapter we discussed about different controllers part and necessity of these controller for the project here we want to do the comparative study of simulation results obtained with different controller used for avoid high temperature system. Before going to simulation results let's see the design model for cascade controller.

I. Setting of Simulation Cases and Comparative Control Laws

Comparative numerical studies were conducted using three methods.

1) C-Fuzzy-PID control law presented in the paper;
2) PID-PID cascade control law, where both the inner fuel oil flow rate loop and outer temperature loop are PID controlled; and
3) PID-Smith cascade control law, where the inner loop uses PID with a Smith predictor and outer loop adopts PID.

In order to realistically simulate the wind tunnel temperature, the target temperature is initially set to 1◦C, and then increased to 2◦C after 50 s. The C-fuzzy-PID control law is evaluated numerically in the following simulation cases.

1) Case A: Temperature responses to step command: To compare the step response of three kinds of control laws, the time lag is set to 0.2 s [see Fig. 6(a)].

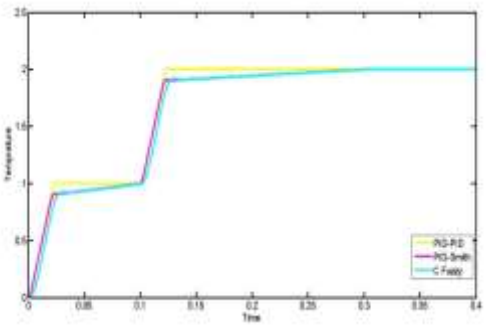

Fig. 8 a) Comparison of step responses

2) Case B: Effect of pure time delay: To investigate the effect of pure time delay in the inner loop flow rate transfer function of the system, the time delay is increased from 0.2 to 0.4 s, while other simulation conditions remain unchanged [see Fig. 6(b)].

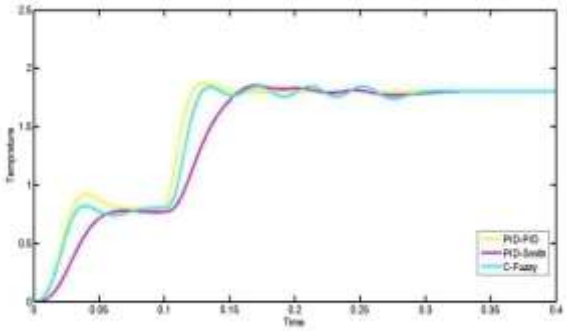

Fig. 8 b) Effect of pure time delay

3) Case C: Effect of working condition (wind speed): Working condition change in wind speed can be characterized by a change in Mach number. An increase in Mach number will result in a decrease in temperature (and vice versa) while the air-fuel ratio is larger than the optimal air-fuel ratio. To examine the effectiveness of handling impact on the system due to a change in wind speed from 0.4 to 0.2 Ma meanwhile keeping other simulation conditions unchanged [see Fig. 6(c)].

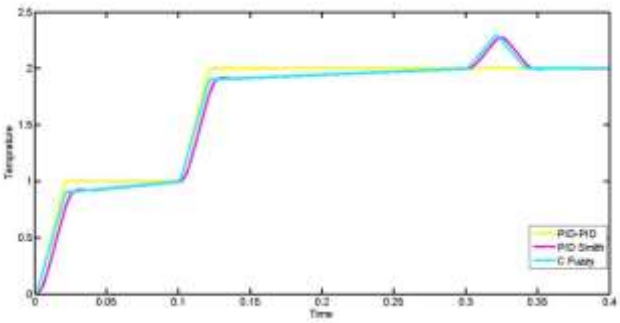

International Journal of Research
Available at https://edupediapublications.org/journals
e-ISSN: 2348-6848
p-ISSN: 2348-795X
Volume 05 Issue 12
April 2018

Fig.6 c) Effect of airflow wind speed

4) Case D: Effectiveness of disturbance rejection: A disturbance, which is set to 0.2 V for the input signal of VFD, is added to the inner loop system at t = 100 s [see Fig. 6(d)]

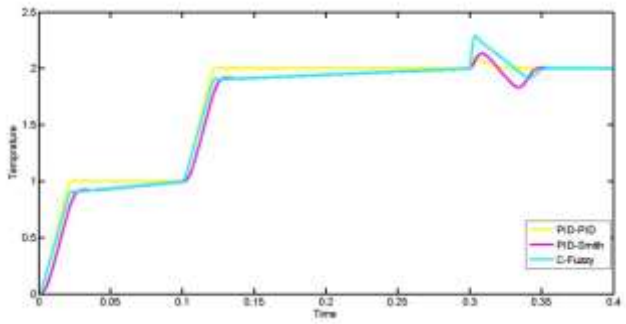

Fig.6 d) Inner Loop disturbance Rejection

Fig.6 Results of comparative studies of three control laws

II Discussions of Simulation

Some observations can be made from the simulated results. As illustrated in Fig. 7(a), although all three methods yield an over damped temperature response to step changes, the fuzzy-PID method significantly improves the response time over both traditional PID-PID and PID-Smith control methods. The PID Smith has a slightly shorter settling time than that of PID-PID as it incorporates Smith predictor to compensate the time lag in the inner loop.

Fig. 6(b) illustrates that an increase in time delay causes an overshoot and lengthens the settling time. The fuzzy-PID controlled system exhibits an excellently short settling time as compared to the PID-PID and PID-Smith cascade control methods despite the fact that it yields a slightly larger overshoot in the response. It is interesting to note that that the PID-PID offers a better transient response (both overshoot and settling time) than that of the PID-Smith method in this case. This is because Smith predictor depends on an accurate mathematical model; the control performance degrades when the plant models experience parameter variations.

V. CONCLUSION AND FUTURE SCOPE

I.CONCLUSIONS

A successfully developed C-Fuzzy-PID control system (with an inner flow rate and an outer temperature control loops) for temperature control of a HAWT has been presented. The plant models for both loops, which have been derived in closed form for a physical HAWT, have been shown to provide a useful basis for simulation analysis and controller design. The proposed C-Fuzzy-PID has been numerically investigated by comparing simulation results against two traditional methods; PID-PID and PID-Smith. The inner loop, which incorporates a predictive control law, effectively overcomes influences of large inertia and transport lag in fuel-oil supply system on the temperature responses. The outer loop, where the compensation coefficients of the fuzzy-PID law for temperature control can be tuned (based on combustion theory and experiences) to reflect work conditions, provides an effective means to suppress the impact caused by a change in wind speeds. The models and the proposed C-Fuzzy-PID law have been validated experimentally showing that the proposed controller not only can realize precise temperature control, but also can quickly suppress influences caused by a change of work conditions, parameter variation, and disturbances on the plant. The temperature fluctuation of the system is less than ± 7 ◦C. Simulation and experimental results have confirmed that the C-Fuzzy-PID control algorithm has strong robustness and excellent adaptability. Suggested future work may include a strict theoretical analysis of the proposed C-Fuzzy-PID for the temperature control of HAWT, which takes into account the perturbation of the controlled plant.

II.FUTURE SCOPE

Future work may lie in the investigation of c-fuzzy PID controller since the interaction among different PID may affect each other. Also, the extension to other control system control problems can be explored. We can also move towards the fuzzy controller whose results can matches with the required response in shorter time period. And concept of avoid high temperature for improvement of time and speed.

ACKNOWLEDGEMENT

We would like to thank anonymous referees for their valuable comments and suggestions to improve the quality of paper.

BIBLIOGRAPHY

[1] S. Zhao, L. Liao, and Y. Chen, “1700◦C Hot wind tunnel for thermal Calibration,” Aviation Meas. Testing Technol., vol. 20, no. 4, pp. 3–6, Apr. 2000.

[2] T. Peng, B. Xu, and H. Yang, “Variable frequency hydraulic technology Development and research,” J. Zhejiang Univ., vol. 38, no. 2, pp. 215–221, Feb. 2004.

[3] T. Zhao, J. Zhang, and L.Ma, “On-line optimization control method based on extreme value analysis for parallel variable-frequency hydraulic pumps in central air-conditioning systems,” Building Environ., vol. 47, pp. 330– 338, Jan. 2012.

[4] H. Yang, W. Sun, and B. Xu, “New investigation in energy regeneration of hydraulic elevators,” IEEE/ASME Trans. Mechatronics, vol. 12, no. 5, pp. 519–526, Oct. 2007.

[5] B. Xu, X. Ouyang, and H. Yang, “Energy-saving system applying pressure accumulators for VVVF controlled hydraulic elevators,” presented at the ASME Int.Mech. Eng.Congr. Expo.Washington, DC, USA, Nov. 16–21, 2003.

[6] B. Xu, J. Yang, and Y. H. Yang, “Comparison of energy-saving on the speed control of VVVF hydraulic elevator with and without pressure.

[7] D. Hu, S. Ding, H. Zhu, B. Xu, and H. Yang, “Velocity-tracking control of the variable-speed controlled hydraulic system: Using compound algorithm of PD & feed-forward-feedback control,” in Proc. 3rd IEEE Conf. Meas. Tech. Mechatronics Autom., 2011, pp. 1109–1116.

[8] R.Manasek, “Simulation of an electro-hydraulic load-sensing system with AC motor and frequency changer,” in Proc. 1st IEEE Conf. FPNI-PhD Symp., 2000, Slovakia, pp. 311–324.